Normal-Mode–Vortex Interactions

R. Bernal, Christophe Coste, F. Lund, F. Melo

Normal-Mode–Vortex Interactions

R. Bernal,[1] C. Coste,[2] F. Lund,[3,4] and F. Melo[1,4]

[1]*Departamento de Física de la Universidad de Santiago de Chile, Avenida Ecuador 3493, Casilla 307 Correo 2 Santiago-Chile*
[2]*Groupe de Physique des Solides, Tour 23-13, 1 er étage, 2 Place Jussieu, 75251 Paris Cedex 05, France*
[3]*Departamento de Física, Facultad de Ciencias Físicas y Matemáticas Universidad de Chile, Casilla 487-3, Santiago-Chile*
[4]*Centro para la Investigación Interdisciplinaria Avanzada en Ciencias de los Materiales (CIMAT), Santiago-Chile*
(Received 12 November 2001; published 25 June 2002)

Standing surface waves that interact with a confined, vertical, vorticity field with zero net circulation are studied both analytically and experimentally. The surface waves are generated by vertical vibration, and constant vorticity injection is achieved by a rotating disk flush mounted in the cell. Experimental results are indicative of a local wave-vortex interaction (no dislocation), and a simple theoretical model is able to explain them in quantitative detail.

DOI: 10.1103/PhysRevLett.89.034501 PACS numbers: 47.32.Cc, 47.35.+i, 67.40.Vs

The interaction of sound and vorticity in homoentropic flows has been the subject of much recent interest [1]. When the flow is unbounded, sound may be scattered by vorticity in a situation such that a Born approximation scheme applies, and there results a linear relationship between scattered acoustic pressure and (Fourier transform of) vorticity. This relation suggests a possible nonintrusive probe of vortical, including turbulent, flows [2]. In addition, conceptually simple but experimentally sophisticated time-of-flight techniques in a geometrical acoustics limit have been used to study a variety of flows [3]. When the flow is bounded, there will be an interaction between the acoustic normal modes of the flow and vorticity, suggesting a possible probe to study turbulence in a confined geometry. The bounded flow may also be a self-gravitating object such as a star, whose normal modes will be affected by the presence or absence of turbulence in its interior [4].

Interesting flows occur both in two and three dimensions. The situation in two dimensions is of particular interest because vortices with nonzero circulation may exist. In that case the Born approximation scheme breaks down and outstanding theoretical issues concerning acoustic scattering have only recently been cleared up both in the long [5] and short [6] wavelength limits. A remarkable result of Berry *et al.* [7] indicating that a vortex of nonvanishing circulation would induce a dislocation on the acoustic wave fronts, much like what happens in the Aharonov-Bohm effect [8] was experimentally verified by Roux *et al.* [9].

Since acoustic wave visualization involves sophisticated techniques, we have undertaken a study of the interaction of vertical vortices with surface waves.

In a recent paper [10], we have reported results on the effect of a localized vertical vortex of nonvanishing net circulation on a propagating surface wave. As expected, the qualitative predictions of Berry *et al.* [7], obtained on the basis of analogies between de Broglie and surface waves, were borne out: in the proper parameter range a dislocation develops on the incident wave, and an additional scattered wave appears. Our experimental setup, however, allowed for a quantitative study of the whole fluid surface, pointing out the importance that boundary conditions at the vortex core have on the resulting symmetry of the scattering problem. Such symmetry problems also have arisen in relation to the scattering of phonons with vortices in superfluids [11]

Vortices in nature may very often have vanishing net circulation. Particularly, vortices arising within turbulent flows in confined geometries, where stationary boundary conditions will impose zero net overall circulation. Since acoustic waves, in the form of normal modes of a resonant cavity, are a particularly attractive way to probe such flows, the question naturally arises of how waves interact with vortices of zero net circulation. This paper reports results that pertain to this issue. It is shown that there exist stationary solutions for the normal modes of a cavity in the presence of localized, stationary circulation, and such solutions are quantitatively characterized, both experimentally and theoretically. Two vortex parameters are easily inferred from this experiment: fluid rotation at the core, and net circulation (vanishing or not).

The easiest way to produce well defined standing surface waves is by vertically vibrating a thin fluid layer [12]. In this situation no net horizontal momentum is injected into the fluid, the normal modes of the layer are parametrically excited and oscillate at half of the excitation frequency. Also, it is well known that the selection of the wavy structure depends mainly on the fluid viscosity [12]; squared patterns appear at low viscosity whereas stripes do at high viscosity. Hexagons and other combinations of standing wave patterns are also possible: for instance quasicrystals have been observed independently of the container shape [12]. In this article only the stripes case is considered quantitatively. In a linear medium, such a pattern can be thought of as a superposition of two equal waves propagating in opposite directions. Herein lies the advantage of exciting the normal modes parametrically rather than by lateral vibration: in this case wave attenuation would make it difficult to balance right going with left going waves.

In our setup a stadium-shaped cell, 200 mm long, 100 mm wide, and 3 mm deep is vertically vibrated. As in many previous experiments, the vibrations are generated by a shaker table (Techron 5515) at frequencies and accelerations that range from 20 to 300 Hz and $0.01g$ to $3g$ respectively. The actual acceleration of the container is measured by a piezoelectric accelerometer (B K 4875) with a resolution of $0.01g$. Wave visualization is achieved by lighting the fluid surface with a ring of 60 equally distributed red LEDs. The ring, 20 cm in diameter, is fixed above the fluid cell at a height of 120 cm. A high speed camera (HISIS 2002) located at the ring center captures the image of the surface. In this way the reflected light from a flat fluid layer defines an angle that is just out of the camera field. When surface waves are excited, the light reflected on the wavy surface can be collected by the camera as caustic lines [13]. Since stripes have a tendency to arrange perpendicularly to the cell borders, the stadium shape cell allows us to produce well-defined and uncompressed stripes in the central region of the container in which measurements are performed. A square container has also been used to obtain stable square patterns, with a low viscosity fluid. Similar results are obtained for both the square and the striped pattern. In both cases, the meniscus due to capillarity are reduced by locating the contact line at the same level as the sharp edge of the container sidewalls.

Confined vorticity is produced by rotating a 5 mm radius disk, flush mounted and centered on the container bottom. Disk speed is controlled by a small dc motor located just underneath. An O-ring is used as a seal to avoid fluid leaking. Vorticity is characterized by a particle tracking method from which surface fluid speed is determined. Figure 1 shows the angular velocity obtained by this method,

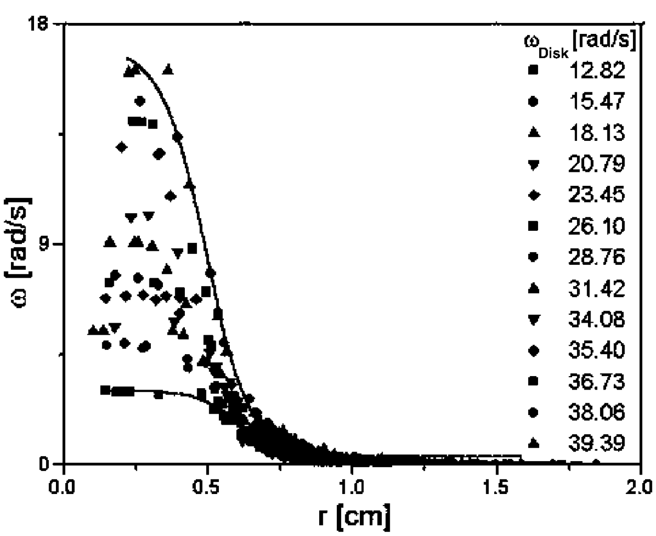

FIG. 1. Velocity distribution at the free water surface for several disk rotation rates ω_{disk}.

for several rotation disk rates. Experimentally, the vortex is well described by a core of radius a ($a \sim 0.43$ mm.) within which the fluid is in solid rotation, surrounded by a region of rapid exponential decrease. This means that, in contrast with the experimental situation studied in [10], the vortex *is not* a topological defect, because its circulation is *not* constant, but rather decreases very rapidly with distance to the center. As we can see in Fig. 2, the effect on the wave fronts is only local, and no dislocated wave is observed away from the vortex core. From Figs. 2(a)–2(c), an inclination of the wave font located on the vortex region is clearly detected. For low rotation rates, the angle of this inclination increases linearly with the vortex frequency. For high rotation rates, as the case illustrated in Fig. 2(d), this angle becomes close to 90° and the wave front exhibits a phase shift on the order of 2π. Similar results are obtained when inverting the vortex rotation, although the pattern tilt is produced on the opposite direction. In addition, the resulting effect of the vortex on the waves is independent of the experimental sequence, i.e., turning on the vortex first, followed by the setting of waves produces the same pattern that the opposite order, i.e., no hysteresis effect is observed. The waves are a small perturbation on the flow of the externally driven vortex. Thus, the flow due to the wave has no significant effect on the vortex. If the vortex frequency was of the order wave frequency, resonances might occur. However, this would entail, in our surface wave experiment, a nearly supersonic vortex, taking us way out of our perturbation regime.

In the following we present a simple theoretical description of the effect the vortex has on the standing surface waves. Our analysis is based on the assumption that it is equivalent to look at the wave instability problem including the vortex on the basic state as studying the vortex effect once the wave pattern is well developed. In other words, in our calculations, the fact that waves are a result of an instability produced by vibrations is just ignored. This approach is obviously valid for low dissipative fluids for which the instability onset can be neglected with respect to gravity. Although the validity of assumption is less obvious for highly viscous fluids, we show below that calculations reproduce the main features of the observed structures.

The interaction between a surface wave on a shallow fluid of local elevation $\eta(r, \theta, t)$, where (r, θ) are polar coordinates, and a stationary, vertical, axially symmetric

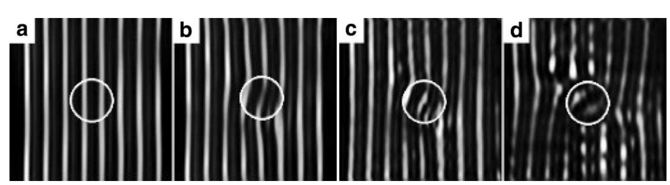

FIG. 2. Snapshot of surface waves at $f = 53$ Hz and $\lambda = 0.43$ cm interacting with a vortex of increasing circulation. In all figures, fluid rotates clockwise. (a) $\omega_{\mathrm{disk}} = 0$; (b) $\omega_{\mathrm{disk}} = 20.8$ rad/s; (c) $\omega_{\mathrm{disk}} = 31.4$ rad/s; (d) $\omega_{\mathrm{disk}} = 38$ rad/s.

velocity field $\mathbf{U}$ is described [14] by the equation derived in Ref. [6], which reads

$$\left(\frac{\partial}{\partial t} - \mathbf{U} \cdot \nabla_\perp\right)^2 \eta - c_\phi^2 \nabla_\perp^2 \eta = 0, \quad (1)$$

where $\nabla_\perp$ is the horizontal gradient and c_ϕ the phase velocity of the surface waves. As in [6], we look for solutions that evolve harmonically (with a single global frequency ν) in time, and Fourier decompose them in the polar angle θ:

$$\eta = \mathrm{Re}\left[\sum_n \eta_n(r) e^{i(n\theta - \nu t)}\right], \quad (2)$$

where Re stands for the real part. Since the velocity field for the vortex is stationary and axisymmetric, $U = U(r)\hat{\theta}$, the function $\eta_n(r)$ obeys an ordinary differential equation:

$$\left[\frac{d^2}{dr^2} + \frac{1}{r}\frac{d}{dr} - \left(\nu^2 - \frac{nU(r)}{r}\right)^2\right]\eta_n = 0. \quad (3)$$

Within the vortex core, the velocity field can be approximated by

$$U(r) = \frac{\omega_0}{2} r \quad \text{for } r \leq a. \quad (4)$$

Injecting this expression in (3), we see that, within the core η_n^c satisfies a Bessel equation, whose solution, finite at the origin may be written

$$\eta_n^c = a_n \frac{J_n(\beta\gamma_n r')}{J_n(\beta\gamma_n)} \quad \text{for } r' \leq 1, \quad (5)$$

where a_n is a numerical constant, $r' \equiv r/a$ is the dimensionless radius, $\beta = ka$ and $k \equiv \nu/c_\phi$ is the wave number. We also introduce the definitions

$$\gamma_n \equiv \left|1 - \frac{n\alpha}{\beta^2}\right|, \qquad \alpha \equiv \frac{\nu\omega_0 a^2}{2c_\phi^2}. \quad (6)$$

Outside the core we choose a simple fit to the experimental velocity field through the following polynomial approximation:

$$U(r) = \frac{\omega_0}{2(\mu^2 - 1)} r\left(\frac{\mu^2 a^2}{r^2} - 1\right) \quad \text{for } a \leq r \leq \mu a, \quad (7)$$

where $\mu > 1$ is a numerical parameter. This form ensures continuity of the velocity at $r = a$, and decreases monotonously toward 0 at $r = \mu a$. We choose the parameter μ in such a way that the approximate and experimental velocity fields both have the same slope at $r = \mu a$. The physical justification of this requirement is that it is the regions of maximum velocity that will have the greatest effect on the vortex, so that it is this region that we seek to accurately model.

The above choice (7) allows for a closed analytical form for the solution of Eq. (3). Indeed, inserting the velocity field (7) into (3), we obtain

$$\left\{\frac{d^2}{dr'^2} + \frac{1}{r'}\frac{d}{dr'} + \left[\beta^2\tilde{\gamma}_n^2 - \frac{m^2}{r'^2}\right]\right\}\eta_n^{\mathrm{inter}}(r') = 0, \quad (8)$$

which is a Bessel equation of order

$$m(\alpha, n, \mu) \equiv \sqrt{n^2 + \frac{2n\alpha\mu^2}{\mu^2 - 1}} \quad (9)$$

whose solution is $(1 \leq r' \leq \mu)$

$$\eta_n^{\mathrm{inter}} = b_n \frac{J_m(\beta\tilde{\gamma}_n r')}{J_m(\beta\tilde{\gamma}_n)} + c_n \frac{H_m^{(1)}(\beta\tilde{\gamma}_n r')}{H_m^{(1)}(\beta\tilde{\gamma}_n)}, \quad (10)$$

where

$$\tilde{\gamma}_n \equiv \sqrt{1 + \frac{2n\alpha}{\beta^2(\mu^2 - 1)}}. \quad (11)$$

Last, we suppose that the velocity $U(r) = 0$ for $r' > \mu$, so that the solution of (1) in this region is simply

$$\eta_n^{\mathrm{out}} = e^{i\beta r'\cos\theta} + d_n \frac{H_n^{(1)}(\beta r')}{H_n^{(1)}(\beta\mu)} \quad \text{for } \mu \leq r'. \quad (12)$$

This solution respects the obvious physical requirement that the wave should be a linear superposition of an outgoing scattered wave (represented by the Hankel function $H_n^{(1)}$) and the incident plane wave. As we said, the vortex is not a topological defect, so that there is no dislocated wave, in contrast with our previous work [6]. The dimensionless parameter α, although with the same definition as before [compare (6) here to Eq. (22) of [6]], no longer quantifies the strength of a dislocation, but indicates the strength of the vortex-wave interaction in the vortex core.

The four unknown constants a_n, b_n, c_n, d_n are determined by requiring the continuity of $\eta(r')$ and its first derivative at the two boundaries $r' = 1$ and $r' = \mu$. This gives four relations which are readily solved, and (5), (10), and (12) give the complete solution of the problem.

Now, if we want the solution in the case of stationary waves interacting with a vortex, we just have to add the solution for an incident plane wave coming from the other side, $e^{-i\beta r'\cos\theta}$, since the wave equation (1) is linear. The comparison of experiments and calculations is made in Fig. 3. Some features of the observations, such as the very localized "tilting" of the wave fronts just at the vortex center are very well reproduced. We see very clearly that the "dislocation" is confined to the immediate neighborhood (one or two wavelengths) of the vortex center, in contrast to the case when the vortex is of constant circulation (see Figs. 1 and 2 of [10]). No free parameters are used in this comparison of theory and experiment: The value of $\beta = 2\pi$ is fixed by the measurement of the wavelength and the vortex radius; α is given [15] by the measured value of the angular velocity of the fluid in the vortex core, and μ is given by the measured value of the slope of the exponentially decreasing velocity at $r = a$. Note that the theoretically calculated field displays the complete interference pattern of the scattered wave with the incident wave, an effect which is not observed experimentally.

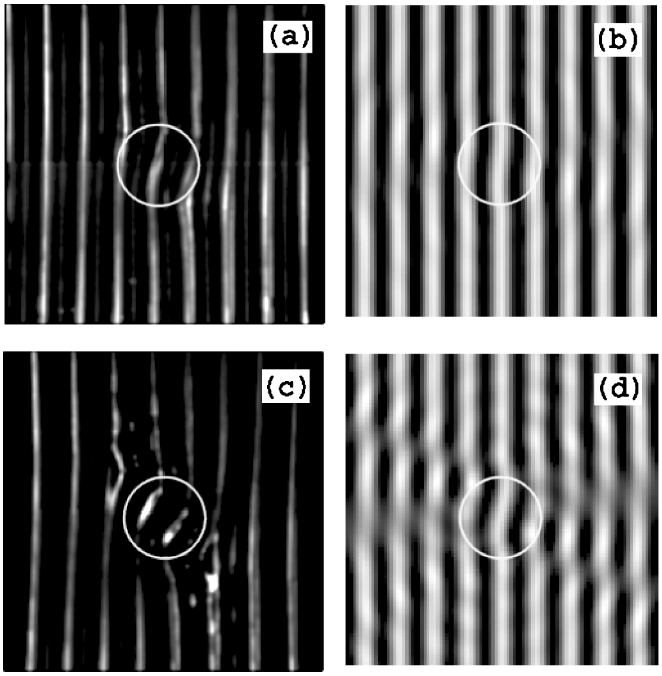

FIG. 3. Comparison between experiments and theoretical predictions. Experimental snapshots [(a), (c)] and corresponding density plot [(b), (d)] of the surface elevation for stationary wave. The two bright regions are separated by a wavelength, the box size is 9×9 in units of wavelength, the vortex is at its center and rotates clockwise. The parameters used in the calculations are $\beta = 2\pi$ (the wavelength is close to the vortex radius), $\alpha = 0.44$ [(b)] and $\alpha = 1.25$ [(d)]. They are calculated from the measurements of the velocity field.

This is not surprising, because the theoretical calculations do not take viscosity into account, whereas experimentally the fluid viscosity has to be large (50 times that of water) in order to obtain stripes as the stable pattern for the stationary waves. The parametric excitation feeds the stationary wave with the energy that it loses during each period of oscillation, and the constant rotation at the bottom of the box maintains the vortex circulation in the core. Thus the plane wave fronts and the tilted ones are stable patterns, but the scattered wave is rapidly damped by viscosity.

One might ask, due the particular boundary conditions introduced, if the stadium shape container plays a role in selecting the stationary pattern we observed. We think that this is not the case since the same qualitative results have been obtained for square pattern. We notice that the square patterns can be seen as the superposition of two standing waves whose wave vectors are at right angles to each other. In this case, for each standing wave we observe a similar tilt.

To conclude, we have studied the interaction of standing waves with vorticity of zero net circulation in a finite cavity. Stationary solutions for the normal modes in the presence of a localized, stationary, vortex were found and characterized, both experimentally and theoretically. The interaction is local, with a tilt that can be satisfactorily explained in terms of local advection by the vortex velocity field.

We gratefully acknowledge the support of Fondecyt Grant No. 1990035 (F. L.), FONDAP Grant No. 11980002 (F. L., F. M.), and ECOS-CONICYT.

[1] For a review, see Proceedings of the 2000 Cargese Summer School "Sound-Flow Interaction" (to be published).
[2] For theoretical aspects, see R. H. Kraichnan, J. Acoust. Soc. Am. **25**, 1096 (1953); M. J. Lighthill, Proc. Cambridge Philos. Soc. **49**, 531 (1953); T. Kambe, J. Jpn. Soc. Fluid Mech. **1**, 149 (1982) (in Japanese); M. S. Howe, J. Sound. Vib. **87**, 567 (1983); A. L. Fabrikant, Sov. Phys. Acoust. **29**, 152 (1983); F. Lund and C. Rojas, Physica (Amsterdam) **37D**, 508 (1989). Experiments include C. Baudet, S. Ciliberto, and J. F. Pinton, Phys. Rev. Lett. **67**, 193 (1991); M. Oljaca *et al.,* Phys. Fluids A **10**, 886 (1998).
[3] P. Roux and M. Fink, Eur. Phys. Lett. D **32**, 25 (1995); R. Labbe and J.-F. Pinton, Phys. Rev. Lett. **81**, 1413 (1998); S. Manneville *et al.,* Eur. J. Phys. B **9**, 545 (1999); S. Manneville *et al.,* Phys. Fluids **11**, 3380 (1999).
[4] For a perspective on Helioseismology, the study of the suns interior through the observed surface oscillations due to resonant sound waves, see P. Demarque and D. B. Guenther, Proc. Natl. Acad. Sci. U.S.A. **96**, 5356 (1999); see also G. Fiorentini, B. Ricci, and F. L. Villante, Nucl. Phys. (Proc. Suppl.) **95**, 116 (2001).
[5] R. Ford and S. Llewellyn Smith, J. Fluid Mech. **386**, 305 (1999).
[6] C. Coste, F. Lund, and M. Umeki, Phys. Rev. E **60**, 4908 (1999); C. Coste and F. Lund, Phys. Rev. E **60**, 4917 (1999).
[7] M. V. Berry *et al.,* Eur. J. Phys. **1**, 154 (1980).
[8] Y. Aharonov and D. Bohm, Phys. Rev. **115**, 485 (1959). For reviews, see I. Olariu and I. I. Popescu, Rev. Mod. Phys. **57**, 339 (1985); M. Peshkin and A. Tonomura, *The Aharonov-Bohm Effect*, Lectures Notes in Physics Vol. 340 (Springer, Berlin, 1989).
[9] P. Roux *et al.,* Phys. Rev. Lett. **79**, 3170 (1997).
[10] F. Vivanco, F. Melo, C. Coste, and F. Lund, Phys. Rev. Lett. **83**, 1966 (1999).
[11] See E. Sonin, cond-mat/0104221 (to be published); D. J. Thouless *et al.,* Phys. Rev. B **63**, 224 504 (2001).
[12] By way of the well-known Faraday instability, a topic that has received much attention in recent years. For a review, see W. S. Edwards and S. Fauve, J. Fluid Mech. **278**, 123 (1994), and references therein.
[13] J. Bechhoefer, V. Ego, S. Manneville, and B. Johnson, J. Fluid Mech. **288**, 235 (1995).
[14] As shown in [6], it is enough to take (1), valid in the shallow water limit, to understand the interaction of vertical vorticity with surface waves on a deeper fluid. These waves are dispersive and the main effect of dispersion is to renormalize the numerical value of the parameter α defined in (6). Thus, we use (1) for simplicity.
[15] As explained in Ref. [6], we use the relevant definition for dispersive waves, that is $\alpha \equiv \nu \omega_0 a^2/(2c_\phi c_g)$, where c_g is the group velocity.